



## Article

# Concentrations and Retention Efficiency of Tire Wear Particles from Road Runoff in Bioretention Cells

Demmelash Mengistu <sup>1,\*</sup> , Claire Coutris <sup>2</sup> , Kim Aleksander Haukeland Paus <sup>1</sup> and Arve Heistad <sup>1</sup><sup>1</sup> Faculty of Science and Technology, Norwegian University of Life Sciences (NMBU), 1432 Ås, Norway<sup>2</sup> Division of Environment and Natural Resources, Norwegian Institute of Bioeconomy Research (NIBIO), 1433 Ås, Norway

\* Correspondence: demmelash.mengistu@nmbu.no

**Abstract:** Bioretention cells are popular stormwater management systems for controlling peak runoff and improving runoff water quality. A case study on a functional large-scale bioretention cell and a laboratory column experiment was conducted to evaluate the concentrations and retention efficiency of bioretention cells towards tire wear particles (TWP). The presence of TWP was observed in all soil fractions (<50 µm, 50–100 µm, 100–500 µm, and >500 µm) of the functional bioretention cell. TWP concentrations were higher (30.9 ± 4.1 mg/g) close to the inlet to the bioretention cell than 5 m away (19.8 ± 2.4 mg/g), demonstrating the influence of the bioretention cell design. The column experiment showed a high retention efficiency of TWP (99.6 ± 0.5%) in engineered soil consisting of sand, silty-sand, and garden waste compost. This study confirmed that bioretention cells built with engineered soil effectively retained TWP > 25 µm in size, demonstrating their potential as control measures along roads.

**Keywords:** stormwater; infiltration; tread wear; pollutants; soil



**Citation:** Mengistu, D.; Coutris, C.; Paus, K.A.H.; Heistad, A.

Concentrations and Retention Efficiency of Tire Wear Particles from Road Runoff in Bioretention Cells. *Water* **2022**, *14*, 3233. <https://doi.org/10.3390/w14203233>

Academic Editor: Jianguyong Hu

Received: 21 August 2022

Accepted: 10 October 2022

Published: 14 October 2022

**Publisher's Note:** MDPI stays neutral with regard to jurisdictional claims in published maps and institutional affiliations.



**Copyright:** © 2022 by the authors. Licensee MDPI, Basel, Switzerland. This article is an open access article distributed under the terms and conditions of the Creative Commons Attribution (CC BY) license (<https://creativecommons.org/licenses/by/4.0/>).

## 1. Introduction

Bioretention cells (also known as stormwater biofilters or rain gardens) have been widely used to manage stormwater from road runoff [1–3]. The objectives of bioretention cells are to reduce peak runoff, improve runoff water quality through infiltration, sedimentation, and sorption processes, increase groundwater recharge, and enhance the aesthetics of the community [4–8]. While their pollutant removal capabilities (e.g., petroleum hydrocarbon, polychlorinated biphenyls, sediments) have been demonstrated in many studies (e.g., [4,9–11], removal efficiencies vary depending on site characteristics, design, implementation, and climatic conditions [12–14]. The hydrological performance of bioretention cells, their plant growth ability, and their pollutant removal efficiency can be optimized using engineered soil [8].

Tire wear particles (TWP) are a major source of microplastics in the environment [15,16] with potentially adverse effects on human health and aquatic and terrestrial ecosystems [17]. However, TWP are seldom found as pure tire particles in the environment because of mineral encrustations from the road surface during abrasion of tire treads; the resulting particles are therefore termed tire and road wear particles (TRWP) [18–20]. The primary entrance to the environment is runoff [15,21], which contains substantial amounts of TRWP [22]. Runoff treatment in bioretention cells removes TRWP, likely through physical filtration [23]. The removal efficiency can be affected by TRWP size, as demonstrated by [9], who studied TRWP ≥ 125 µm and showed decreasing removal efficiency with decreasing size. This can be problematic for efficient TRWP retention by bioretention cells because significant amounts of smaller TWP (≤50 µm) have been found in road dust [18,24]. The effective removal of microplastics has also been reported in bioretention cells. For example, [9,23] demonstrated a reduction of 91% of microplastic particles >125 µm in bioretention cells. Furthermore, [23] showed high removal (84%) of microplastic particles

>106  $\mu\text{m}$ , including rubber fragments, in bioretention cells, while [25] reported >70% removal for larger microplastics and TRWP (>100  $\mu\text{m}$ ), and [26] showed >90% removal of TRWP between 20 and 100  $\mu\text{m}$  in vegetated bioretention and 60% in non-vegetated filters.

The main objective of this study was to evaluate whether bioretention cells established with engineered soil retain TWP from road runoff, including finer TWP sizes. More specifically, this study aims to (1) identify and quantify TWP concentrations retained in different soil size fractions of bioretention cells (functional bioretention cells and lab-scale columns) and (2) evaluate the TWP retention efficiency and TWP concentrations in the top and bottom 5 cm of the column soil.

## 2. Materials and Methods

### 2.1. Case Study

#### 2.1.1. Sampling Site and Sample Collection

A case study was conducted on a bioretention cell in Drammen, Southern Norway. The bioretention cell was established in 2019 using engineered soil (70% sand, 30% garden waste compost, size fractionation in Table 1) and designed to optimize hydrological conditions (lower peak flow) and plant growth [27]. The bioretention cell is located on a street with a speed limit of 50 km/h and a traffic density of 20,800 annual average daily traffic (AADT) [28]. It receives road runoff through several standardized inlets fitted to the side curb, a 13 cm high structure separating the driveway from the bioretention cell (Figure 1). These inlets are 70 m apart; they operate only during the warmer seasons and are closed during the cold winter season owing to icing (December–March) [27].

**Table 1.** Proportion (by mass) of each soil fraction in bulk soil collected from a functional bioretention cell in Drammen, Norway, close to the inlet (A) and 5 m away from it (B).

Soil Size Fraction ( $\mu\text{m}$ )	Proportion in Bulk Soil (%)	
	A	B
<50	3.8	3.3
50–100	24.6	22.6
100–500	35.6	39.0
>500	36.0	35.1



**Figure 1.** Left picture: the bioretention cell is the area located between the road and the sidewalk. Right picture: inlets specially designed and fitted to the side curb bring road runoff to the bioretention cell. A 13 cm high side curb (a) separates the road from the bioretention cell. Sampling spot in front of an inlet (b).

Topsoil samples (0–5 cm) were collected in April 2021 using a soil-sampling tube. Samples were collected from six different locations: three spots, each located directly in front of three different inlets and three spots each located 5 m away from these inlets. The samples were oven-dried at 105 °C for 24 h. Samples collected at the inlets were mixed and homogenized using a not sharp-edged Kenwood kitchen blender KMM770 (Kenwood, Havant, Hampshire, UK) for 5 min at high speed to prepare a composite sample A. The three samples taken 5 m away from the inlets were mixed and homogenized similarly, resulting in composite sample B.

### 2.1.2. Size Fractionation

After sieving soil samples with a 5 mm mesh to exclude materials beyond the range of defined microplastics, 30 g of composite samples A and B was sifted using a vibratory sieve shaker (Retac 3D, Retsch, Germany), with stainless steel mesh sizes of 50, 100, and 500 µm. The four fractions collected (<50 µm, 50–100 µm, 100–500 µm, >500 µm) were weighed using an analytical balance AT200 METTLER, (Mettler-Toledo GmbH, Giessen, Germany) and the proportion of each size fraction was determined by dividing the mass of the specific size fraction by the total mass recovered after sieving. Mass recovery of the size fractionation after dry sieving of 30 g of soil sample was 99% for sample A and 97% for sample B. The proportion of each soil fraction in the bioretention soil was similar close to the inlet and 5 m away from it, with 72 and 74% of particles >100 µm, respectively (Table 1).

The coarser fraction >500 µm was crushed with a mortar and pestle to increase the homogeneity. All samples were then analyzed in triplicate using simultaneous thermal analysis coupled with Fourier transform infrared spectrometry (STA-FTIR), followed by parallel factor analysis (PARAFAC) data modeling, as described in Section 2.3. Differences in TWP concentrations across size fractions and sampling sites were analyzed using a two-way analysis of variance, followed by a Tukey pairwise comparison test to identify different concentrations. The total TWP concentration in bulk soil was first estimated by factoring concentrations in each size fraction by the soil size fraction proportion (%) (Table 1) in a bulk sample and then adding concentrations in all size fractions. Differences in total TWP concentrations between groups A and B were analyzed using *t*-tests.

## 2.2. Column Experiment

### 2.2.1. Engineered Soil and Column Dimensions

An engineered soil was prepared in the laboratory, by mixing medium sand, silty sand, and garden waste compost collected at Lindum AS, Norway, at a ratio of 8:15:6 by mass. This engineered soil was recommended by [27] because of its infiltration efficiency and quality in promoting plant growth [29]. The physical and chemical properties of the soil used in this experiment were analyzed in a commercial laboratory, Eurofins, (Moss, Norway), and are presented in SI1. Three similar cylindrical columns ( $C_1$ ,  $C_2$ ,  $C_3$ , diameter 3.8 cm, surface area 11.34 cm<sup>2</sup>, and height 50 cm) were each filled with 40 cm of engineered soil. Dry packing of the columns was used: air-dried soil was added with a funnel into the columns and then gently pressed by hand. The column test was configured based on the dimensional parameters of the functional bioretention cells [3]. The ratio of the column diameter to the effective grain size (see Figure S1 for grain size distribution) was greater than the recommended minimum ratio (50:1) to avoid wall effects [30]. The bottom of the column was sealed with a lid with two small openings (5 mm in diameter) to release effluent water. The openings were connected to a 20 L container to collect the effluent water.

### 2.2.2. Influent Water and Hydraulic Load

Road runoff was collected in April 2021 from two gully pots in Ås, Southern Norway, serving as influent water to the columns. The presence and concentration of TWP in the sediments of these gully pots (Sjorskogenveien and Raadhusplassen) were demonstrated and studied in detail by [31]. Standing water and sediments from the gully pots (120 L from Sjorskogenveien and 100 L from Raadhusplassen) were collected and stored in a cold

room. During application to the columns, the water was continuously stirred to keep the particles in suspension, and applied similarly to the three columns ( $C_1$ ,  $C_2$ , and  $C_3$ ) using Watson peristaltic pumps, calibrated to yield a hydraulic load of 3.7 mm/min for 10 min (total water height of 37 mm). The application rate and duration were chosen to represent a Norwegian water quality design rain for a bioretention cell, sized to collect and treat runoff from a catchment 10 times the size of the bioretention cell area [32]. The pumps were programmed for 10 min on and 30 min off (10 min application, 30 min rest). The resting period was later prolonged (up to 4 h), as the high particle loads caused clogging of the soil and therefore reduced infiltration.

### 2.2.3. Retention Efficiency of the Columns

The TWP retention efficiency of the columns was calculated by analyzing the TWP concentrations in the influent and effluent water. For each of the three columns, 6 L of influent and their entire effluent (13.8 L, 10.3 L, and 14.2 L from  $C_1$ ,  $C_2$ , and  $C_3$ , respectively) were filtered using a 25  $\mu\text{m}$  mesh, and the retained particles were dried and analyzed in triplicates using STA-FTIR and PARAFAC, as described in Section 2.3, to determine TWP concentrations.

### 2.2.4. TWP Concentrations in Top and Bottom Soil

At the end of the experiment, the columns were left to drain for 24 h before topsoil (top 5 cm) and bottom soil (bottom 5 cm) were collected. Soil samples were oven-dried at 105 °C and subjected to density separation using 1.8 g/cm<sup>3</sup> ZnCl<sub>2</sub> solution for 2 h, to get rid of heavier soil particles. As the particle density of TRWP is estimated to be 1.8 g cm<sup>-3</sup> [33], they float in ZnCl<sub>2</sub> solution; the supernatant was decanted, rinsed with water on 25  $\mu\text{m}$  mesh, and oven-dried at 105 °C. For one of the three columns,  $C_3$ , soil samples were divided into three subsamples, where the first ( $C_3$ ) received the above-mentioned treatment, the second ( $C_3^*$ ) was analyzed without any pretreatment, and the third ( $C_3^{**}$ ) was filtered through a 25  $\mu\text{m}$  mesh without density separation (only particles >25  $\mu\text{m}$  were kept for analysis). Rubber material (RM) and TWP concentrations in the top 5 cm soil and bottom 5 cm soil were calculated. The differences in TWP concentrations at the top 5 cm and bottom 5 cm were analyzed using a *t*-test.

## 2.3. STA-FTIR Analysis and Data Modeling

Decomposition of FTIR data of environmental samples using a valid PARAFAC model provides a mechanism to detect and quantify RMs among many components [34]. Suitable data (thermal and FTIR spectra) of the samples were generated using a simultaneous thermal analyzer STA 449 F1 Jupiter with carrier type S (Netzsch, Selb, Germany), and a Bruker Tensor 27 FTIR spectrometer with an external gas cell (Bruker, Billerica, MA, USA) using the procedure described by [31]. The STA registered changes in mass during pyrolysis, as samples were heated from 40 to 800 °C and released gases to the FTIR. The FTIR scanned spectra of a wavenumber range between 4000 and 600 cm<sup>-1</sup> for gas released from the STA with a resolution of 1.93 cm<sup>-1</sup>, generating 1762 signal points. The FTIR data yielded in 666 spectra per sample, giving a total of 1.1 million data points per sample. The data were arranged in a trilinear multi-way dataset as outlined in [31], to suit PARAFAC [35]. PARAFAC models were then built with components ranging from 2 to 5 using MATLAB (The MathWorks, Inc., R2018a, Natick, MA, USA) and a PLS Toolbox for MATLAB version 8.6 (Eigenvector Research, Inc., Wenatchee, WA, USA). The PARAFAC analysis steps and model validation used were described by [31].

From a valid PARAFAC model, the scores of components identified as RMs, core components of tires [36] and suitable TWP markers [21], were used to calculate the concentration of RMs [31] using Equation (1). The method detection limit (MDL) was 0.7 mg RM per g dry sediment, equivalent to 1.1 mg/g for TWP [31].

$$RM_j = (ml \times a_{if}) / (m \times S_i) \quad (1)$$



where

$RM_j$  = concentration of RM (mg/g)

$ml$  = sample mass loss during pyrolysis (mg)

$m$  = initial sample dry mass (g)

$a_{if}$  = score of the  $f$ th component of sample  $i$  extracted from PARAFAC

$S_i$  = sum of score of components of sample  $i$

RM constitutes a variable but significant fraction of TWP, usually between 40 and 60% [37,38]. In this study, 58% was used based on the most relevant data in the context of the study ([39], tire crumb producer). TWP concentrations were then calculated by dividing RM concentrations by 0.58. Estimation of TRWP concentrations (i.e., taking mineral encrustations into account) was not considered in this study, as a wide range (10–75%) of TWP to TRWP ratios is reported in the literature [18,24,40–42], making TRWP estimation problematic.

### 3. Results and Discussion

#### 3.1. Case Study

##### 3.1.1. Detection of TWP in the Soil of Bioretention Cells

Fitting the STA-FTIR data from all field samples in PARAFAC with three components after a preprocessing of filtering and diskiping resulted in a model that captured 85% variation, had 82% core consistency (Figure S2a) and 88% similarity in split-half analysis (Figure S2b). Models with similar figures of merit are considered valid [43,44]. The spectral signals from the wavenumber and temperature loadings of one of the components mimicked the properties of RM (Figure 2), a typical TWP marker [34]. This result confirms the presence of TWP in bioretention cells receiving road runoff and is consistent with the results obtained by [9,23,25,26], who reported the retention of rubbery fragments in bioretention cells.

##### 3.1.2. TWP Concentrations in Soil Size Fractions Close to and Further away from the Inlet

TRWP sizes are important factors in determining their environmental fate [33,45]. In this study, TWP was observed in all soil fractions (<50  $\mu\text{m}$ , 50–100  $\mu\text{m}$ , 100–500  $\mu\text{m}$ , >500  $\mu\text{m}$ ) of the bioretention cells (Figure 3). TWP concentrations in the soil (in mg per g soil dry weight) were found to differ significantly across size fractions ( $F_{3,16} = 3.76$ ,  $p < 0.001$ ) in A and B.

However, because of the differences in the proportion of soil size fractions in a bulk sample (Table 1), the TWP concentrations of each size fraction were different from those presented in Figure 3. The calculated TWP concentrations in each soil fraction and the total TWP concentrations are presented in Figure 4. The results showed that TWP concentrations in the finer soil fraction (<50  $\mu\text{m}$ ) were significantly lower than those in any of the coarser soil fractions, regardless of the sampling distance from the inlet ( $F_{3,16} = 20.7$ ,  $p < 0.001$ ), except in B where the difference between <50  $\mu\text{m}$  and 100–500  $\mu\text{m}$  was not significant. This is related to the mass of the engineered soil in this fraction (3.8 and 3.3% in A and B, respectively) compared with the other three coarser fractions (Table 1).

Studies on the size distribution of TWP retained by bioretention are scarce. However, the results of the present study are in contrast with those of [46], who covered size ranges up to 500  $\mu\text{m}$  and found a decreasing trend of the TRWP concentrations with increasing sediment grain size in a sedimentation basin. The observed trend in TRWP concentration in the sedimentation basin differed from that found in the street dust analyzed in the same study, which showed no clear trend with size. [46] attributed the observed change in TRWP from coarse in runoff to fine in the sedimentation basin to processes such as easy transportability of finer particles, sedimentation of coarse particles before entering the sedimentation basin, and mechanical degradation of coarse particles. The present study, with bioretention cells close to the road, may not be affected by the processes listed above and may receive similar TRWP as present in road dust, suggesting significant amounts of TRWP below 100  $\mu\text{m}$  entering the bioretention cell. Another study by [47], covering size

ranges similar to those of the present study (but with a lower limit at 10  $\mu\text{m}$ ), showed no clear trend but a relatively higher styrene-butadiene rubber (a TWP marker) concentration in a street runoff in the size fraction  $>500 \mu\text{m}$  than in the size fraction 100–500  $\mu\text{m}$ . However, the studied matrices, street runoff in [47] and bioretention soil in the current study, are different and thus not directly comparable.

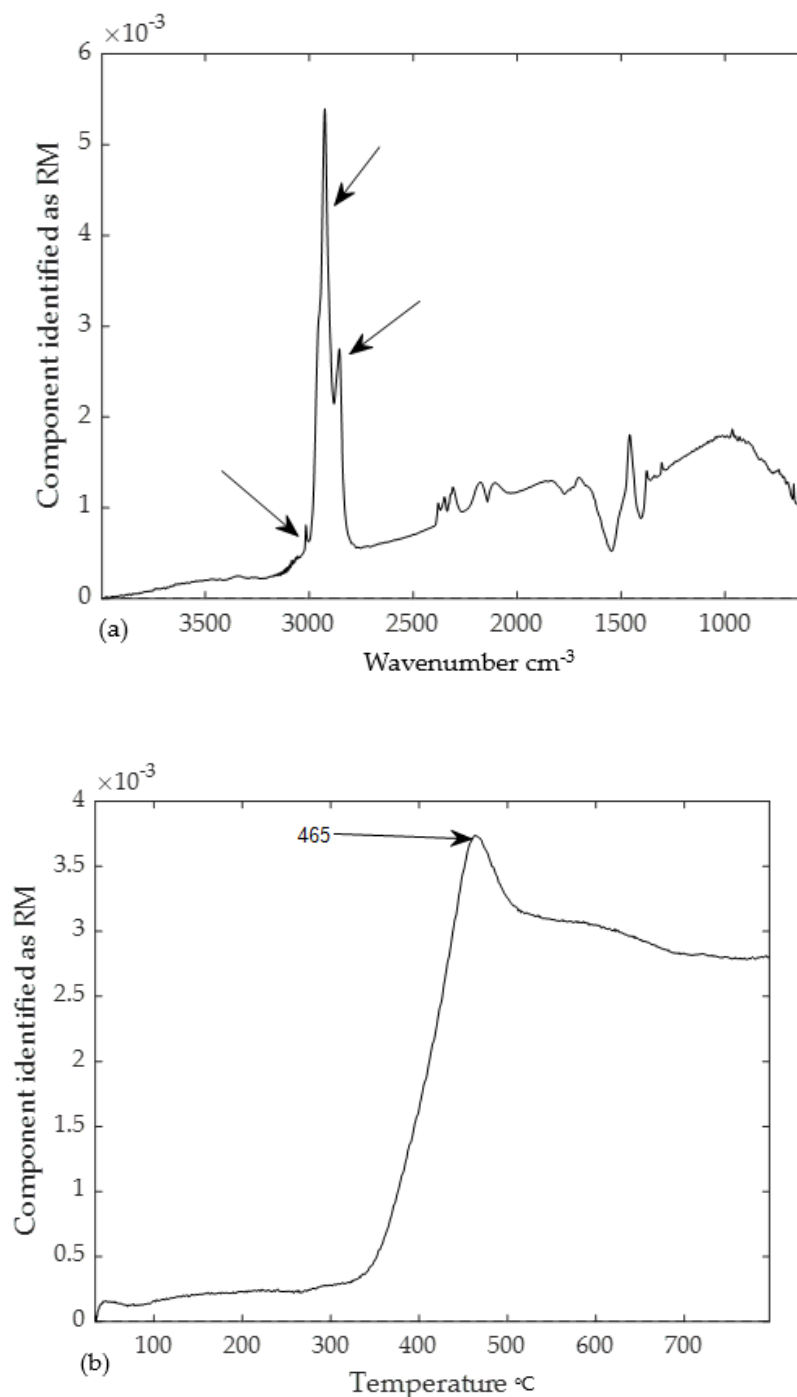


**Figure 2.** Wavenumber (a) and pyrolysis temperature (b) loadings from the rubber materials (RM) component in the PARAFAC model. Peaks supporting the identification of RM are indicated with arrows on the graphs.

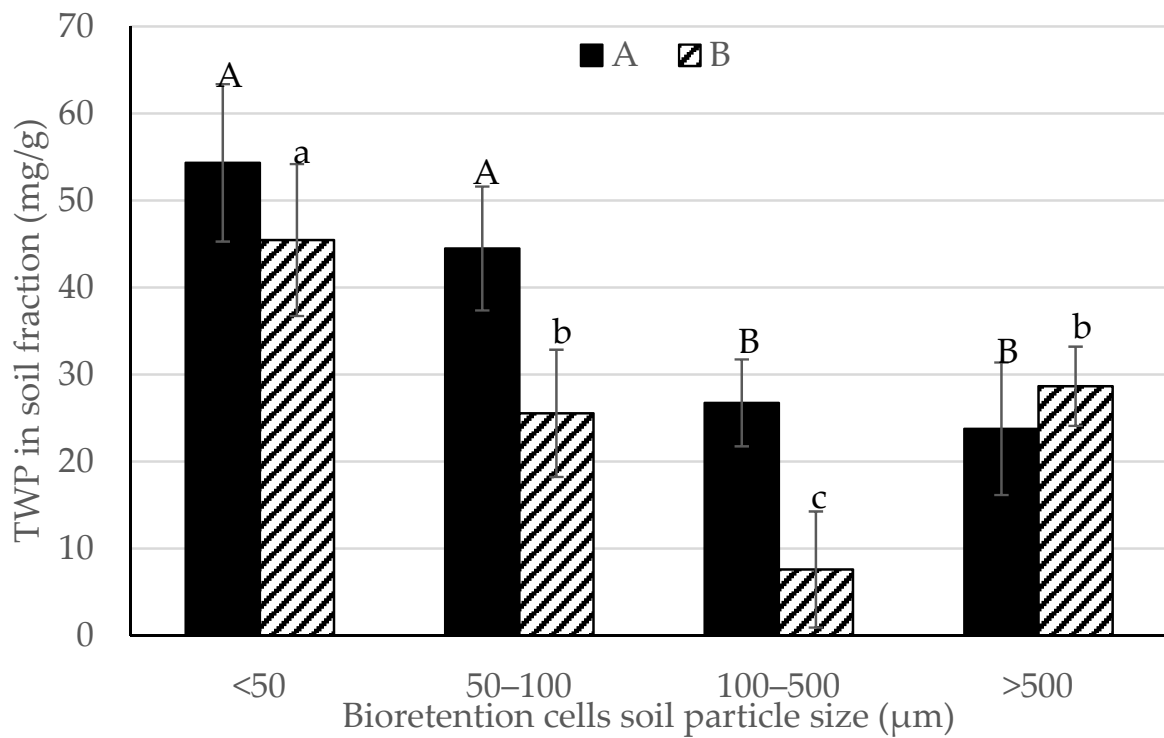


**Figure 3.** Tire wear particles (TWP) concentrations (mg/g, mean and one standard deviation, n = 3) per soil particle size range in soil samples collected from a functional bioretention cell in Drammen, Norway, at the inlet (A), and 5 m away from it (B). Means with different letters are statistically different (Tukey,  $p < 0.05$ ).

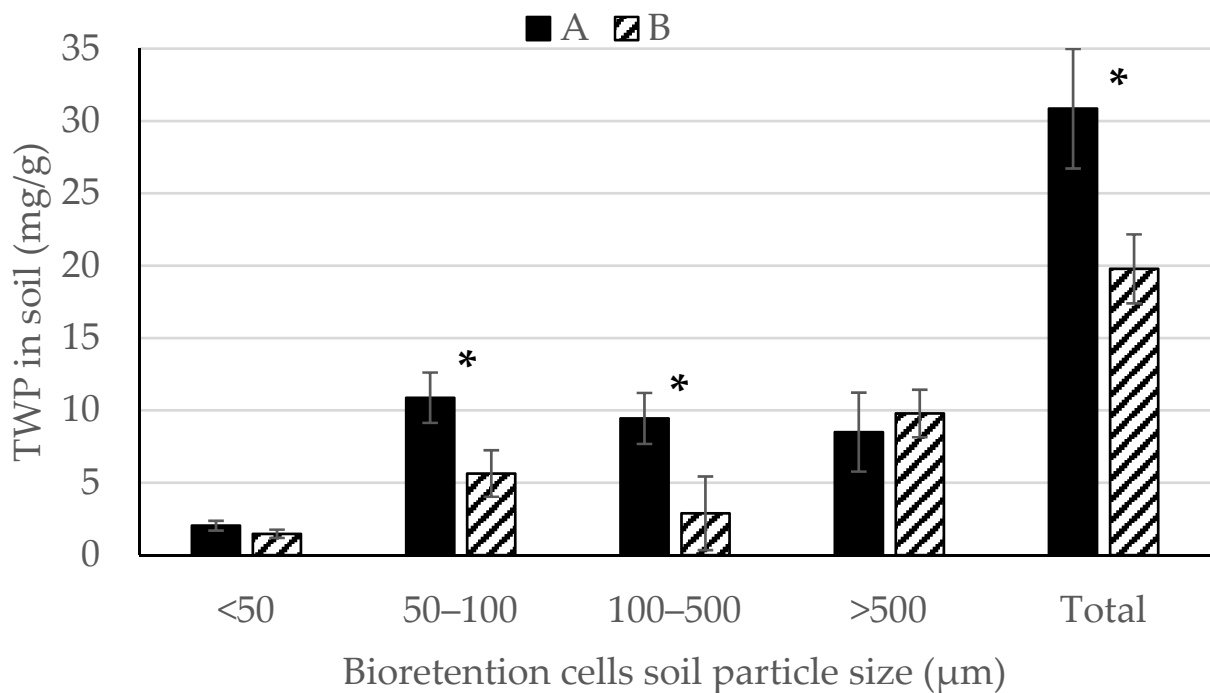


**Figure 4.** Tire wear particles (TWP) concentrations (mg/g, mean and one standard deviation, n = 3) factored by soil size proportion and total TWP concentrations in soil collected from a functional bioretention cell in Drammen, Norway, at the inlet (A), and 5 m away from it (B). Asterisks indicate significant differences between A and B ( $t$ -test,  $p < 0.05$ ).

Retention efficiency could not be assessed because of a lack of data on the incoming and outgoing TWP concentrations. Therefore, it was unclear if the low contribution from the size range  $<50\ \mu\text{m}$  was attributable to a lower share of small-sized TWP entering the bioretention cell, or if the bioretention cell was less efficient in retaining the finer TWP, as reported by [9]. The latter is plausible for two reasons. First, field and road simulator studies have reported that significant amounts of TWP are found in the size range  $\leq 50\ \mu\text{m}$  [18,24]. Second, the main retention mechanism in bioretention cells is physical straining [23], which may allow the transfer of finer TWP down the soil profile or farther away with stormwater. Studies related to the retention efficiency of TWP in bioretention cells are scarce for direct comparison, and the few available studies are based on particle counts. For example, [9] observed up to 100% retention of microplastic particles (including rubbery fragments) larger than  $500\ \mu\text{m}$ . The retention efficiency decreased to 55% for the size fraction between  $125\text{--}355\ \mu\text{m}$ , supporting the suggestion that finer TWP particles may have moved down or away with stormwater.

Total TWP concentrations in mg per g soil dry weight (dw) (all soil fractions considered) were  $30.9 \pm 4.1\ \text{mg/g}$  (mean  $\pm$  standard deviation, SD) at the inlet and  $19.8 \pm 2.4\ \text{mg/g}$  5 m away from the inlet. These concentrations were three and two times higher than the average TWP concentrations reported by [41] in roadside soils in the Seine River watershed, France. The slightly lower TWP concentrations reported in [41] may be attributed to the fact that the roadside soil was sampled at a depth of 0–15 cm (0–5 cm in the present study) and further away from the road edge (3–15 m). However, other factors not specified in the study (e.g., traffic density and service time) make comparisons difficult. [48] estimated an average TWP concentration of  $20.2\ \text{mg/g}$  in roadside soil collected at 0–10 cm depth and 0.5 m away from the edge of federal roads in Germany, with an average traffic density of 24,000 AADT. This is consistent with the TWP concentrations observed in the present study. Although these studies have different TWP-generating conditions and treatment systems than the present study, the results indicate that roadside bioretention systems retain TWP. Not unexpectedly, we also showed that total TWP concentrations in soil, while of the same order of magnitude, were significantly higher at the inlet than 5 m away from it (*t*-test,  $p = 0.03$ ).

### 3.2. Column Infiltration Experiment

#### 3.2.1. Retention Efficiency of the Engineered Soil

An average of  $12.8 \pm 2.1\ \text{L}$  of road runoff with a TWP concentration of  $77.2 \pm 4.9\ \text{mg/L}$  passed through each column (Table 2). With a concentration of solid particles  $>25\ \mu\text{m}$  of  $367\ \text{mg/L}$ , the influent was within the range of total suspended solids concentrations reported in highway stormwater (49–980 and 8–810 mg/L [49,50]). The physical and chemical properties of the soil used in this experiment fulfilled the requirements of bioretention applications with respect to infiltration and plant growth (Supplementary Materials Section S1). However, clogging at the column top was observed after one week of infiltration, suggesting that the initial resting period was insufficient for the hydraulic load and was therefore increased. Particle deposition, which was expected to be high in road runoff, was likely the cause of the clogging. [51] demonstrated clogging at the top of a column owing to particle deposition. Similarly, [52] found a high infiltration decline owing to clogging as a result of sediment accumulation. However, the results of the present study should be interpreted cautiously because a year and a half worth of rainfall was applied for two weeks in the column experiment. Further studies testing the influence of hydraulic loadings on the retention capacity of bioretention cells towards TRWP would be valuable, especially since high TRWP concentrations could hinder the functionality of bioretention cells. Furthermore, the absence of freeze–thaw cycles and vegetation in the columns may have made the soil more prone to clogging than what is typically observed in operative bioretention cells, which also calls for further tests using vegetated columns.



**Table 2.** Tire wear particles (TWP > 25 µm) concentrations in the influent and effluent of bioretention columns (C<sub>1</sub>–C<sub>3</sub>).

Sample	Column	Water (L)	Total Solid Particles >25 µm (mg/L)	TWP Concentration mg/L		Removal Efficiency (%)	
				Mean	SD	Mean	SD
Influent			366.7	79.9	4.9		
Effluent	C <sub>1</sub>	13.8	40.6	0.1	0.1	99.9	0.1
	C <sub>2</sub>	10.3	117.3	0.8	0.2	99.0	0.2
	C <sub>3</sub>	14.2	12.5	0.1	0.0	99.9	0.0

Concentrations of total solid particles >25 µm and TWP >25 µm are listed in Table 2. The effluent contained  $56.8 \pm 54.2$  mg/L of total solid particles >25 µm, with differences observed between columns, which may be attributed to, e.g., heterogeneity of soil compaction and particle concentrations in the influent. Despite this unexpected variability in total solid particles >25 µm in the effluent, the overall TWP removal efficiency remained similar and was  $99.6 \pm 0.5\%$  for TWP > 25 µm. This level of removal is high compared with that of the few available studies on the removal efficiency of microplastics (including rubber fragments) by bioretention cells [9,23,25,26]. However, these studies were conducted on field bioretention cells, which have been in operation for 2–3 years. The bioretention cells had different configurations than the column test in the current study, either in terms of the size of the catchment area they served or in their soil composition.

### 3.2.2. Vertical Distribution of TWP in the Columns

In this study, a test with samples that received no pretreatment, C<sub>3</sub><sup>\*</sup>, showed a TWP concentration of  $5.0 \pm 1.4$  mg/g in the top 5 cm of the column, while the TWP concentration in the bottom 5 cm was below MDL (1.1 mg/g) (Table 3). The relatively high TWP concentration in the top 5 cm seems to originate mainly from the deposition of finer particles (<25 µm), as wet sieving of the same sample with a 25 µm mesh (C<sub>3</sub><sup>\*\*</sup>) showed a reduction in TWP concentration (Table 3). It is likely that these fine particles also contributed to the observed reduction in infiltration in the columns.

**Table 3.** Tire wear particles concentrations (TWP, in mg/g soil dw) in the 0–5 cm (Top 5 cm) and 35–40 cm (Bottom 5 cm) soil layers of bioretention columns C<sub>1</sub>–C<sub>3</sub>, following ZnCl<sub>2</sub> density separation of soil samples. In column C<sub>3</sub>, TWP concentrations were also determined without prior filtration nor density separation (C<sub>3</sub><sup>\*</sup>), and with filtration only (C<sub>3</sub><sup>\*\*</sup>). N/A: not available.

Column	Top 5 cm		Bottom 5 cm	
	Mean	SD	Mean	SD
C <sub>3</sub> <sup>*</sup>	5.0	1.4	0.0	0.0
C <sub>3</sub> <sup>**</sup>	1.0	1.7	N/A	N/A
C <sub>1</sub>	0.9	1.0	0.4	0.5
C <sub>2</sub>	0.8	0.3	0.9	0.5
C <sub>3</sub>	0.6	0.7	0.4	0.2

TWP concentrations, determined in samples pretreated with density separation and filtration, in the top 5 cm ( $0.7 \pm 0.7$  mg/g) and bottom 5 cm ( $0.6 \pm 0.4$  mg/g) showed no statistically significant difference (*t*-test, *p* = 0.21). Considering the mass balance in the influent and effluent, sample pretreatment by density separation may have underestimated TWP concentrations due to unrecovered particles with higher density (>1.8 g/cm<sup>3</sup>). Higher TWP concentrations in the filtered top 5 cm sample (C<sub>3</sub><sup>\*\*</sup>,  $1.0 \pm 1.7$  mg/g) than in the density separated top 5 cm (C<sub>3</sub>,  $0.5 \pm 0.4$  mg/g) also support this suggestion. This result indicates that while sample preparation by density separation using ZnCl<sub>2</sub> is a common

practice in microplastics and TRWP analysis [53–55], it is not optimal for TRWP, as it fails to recover TRWP denser than  $1.8 \text{ g/cm}^3$ . Although comparing TWP concentrations at the top and bottom of the columns provided valuable results, further studies looking at TWP concentrations over the entire soil profile would enable mass balance and thereby a better understanding of TWP fate in bioretention cells.

The results of these experiments imply that bioretention cells are efficient in retaining TWP  $> 25 \mu\text{m}$ . However, the observed high concentrations of TWP  $< 25 \mu\text{m}$  in the top 5 cm of the engineered soil suggests the entry of a high proportion of finer TWP to the bioretention system (Table 3). This warrants further study on the fate of TWP  $< 25 \mu\text{m}$  and their retention by bioretention cells, especially since our results on a large-scale functional bioretention cell showed that TWP in the finer soil fraction ( $< 50 \mu\text{m}$ ) only represented 7% of the top 5 cm of soil.

#### 4. Conclusions

This study demonstrated that bioretention cells built for high infiltration and good plant growth conditions could retain TWP. A case study on a functional bioretention cell showed the presence of TWP in the top 5 cm of soil in all soil size fractions ( $< 50 \mu\text{m}$ ,  $50\text{--}100 \mu\text{m}$ ,  $100\text{--}500 \mu\text{m}$ ,  $> 500 \mu\text{m}$ ). TWP concentration was affected by the inlet fitted to the roadside curb, as TWP concentrations at the inlet were higher ( $30.9 \pm 4.1 \text{ mg/g}$ ) than those observed 5 m away from the inlet ( $19.8 \pm 2.4 \text{ mg/g}$ ).

The column experiment, despite varying concentrations of total solid particles  $> 25 \mu\text{m}$  in the effluent, showed high retention efficiency ( $> 99\%$ ) of TWP  $> 25 \mu\text{m}$  in engineered soil consisting of sand, silty-sand, and garden compost.

The TWP was observed at the top and bottom of the column. Surface clogging and limited infiltration were observed during the experiment and attributed to a high particle load in a short time. A long-term study on a vegetated bioretention cell may provide more realistic wetting and drying conditions and particle loadings from the road environment to better explain the TWP dynamics in bioretention cells. A filter size smaller than  $25 \mu\text{m}$  might also help in understanding the efficiency of bioretention cells in retaining finer TWP. Finally, bioretention cells built with engineered soils not only transport high amounts of runoff water but also have been shown to retain TWP, demonstrating their potential as control measures along roads.

**Supplementary Materials:** The following supporting information can be downloaded at: <https://www.mdpi.com/article/10.3390/w14203233/s1>, Section S1: Particle size distribution of engineered soil; Figure S1: Grain size distribution of the engineered soil used in the column experiment; Section S2: PARAFAC model validity indicators; Figure S2: (a) core consistency of 82%, (b) similarity measure of splits 88%.

**Author Contributions:** D.M.: Conceptualization; Formal analysis; Methodology; Writing—original draft; C.C.: Conceptualization; Funding acquisition; Writing—review and editing; K.A.H.P.: Writing—review and editing; A.H.: Conceptualization; Supervision. All authors have read and agreed to the published version of the manuscript.

**Funding:** Funding from the Norwegian Research Council (Grant number 194051) is gratefully acknowledged.

**Data Availability Statement:** The research data is stored at Norwegian Centre for Research Data. <https://dmp.nsd.no/> (accessed on 21 August 2022).

**Acknowledgments:** The authors wish to thank Monica Fongen for the STA-FTIR analysis of the samples.

**Conflicts of Interest:** The authors declare no conflict of interest.

#### References

1. Ding, B.; Rezanezhad, F.; Gharedaghlou, B.; Van Cappellen, P.; Passet, E. Science of the Total Environment Bioretention cells under cold climate conditions: Effects of freezing and thawing on water infiltration, soil structure, and nutrient removal. *Sci. Total Environ.* **2019**, *649*, 749–759. [CrossRef]

2. Paus, K.H.; Morgan, J.; Gulliver, J.S.; Leiknes, T.; Hozalski, R.M. Assessment of the Hydraulic and Toxic Metal Removal Capacities of Bioretention Cells After 2 to 8 Years of Service. *Water Air Pollut.* **2014**, *225*, 1803. [CrossRef]
3. Kratky, H.; Li, Z.; Chen, Y.; Wang, C.; Li, X.; Yu, T. A critical literature review of bioretention research for stormwater management in cold climate and future research recommendations. *Front. Environ. Sci. Eng.* **2017**, *11*, 16. [CrossRef]
4. Khan, U.T.; Valeo, C.; Chu, A.; Van Duin, B. Bioretention cell efficacy in cold climates: Part 2—Water quality performance. *Can. J. Civ. Eng.* **2013**, *39*, 1222–1233. [CrossRef]
5. Kim, H.; Seagren, E.A.; Davis, A.P. Engineered Bioretention for Removal of Nitrate from Stormwater Runoff. *Water Environ. Res.* **2003**, *75*, 355–367. [CrossRef]
6. LeFevre, G.H.; Paus, K.H.; Natarajan, P.; Gulliver, J.S.; Novak, P.J.; Hozalski, R.M. Review of Dissolved Pollutants in Urban Storm Water and Their Removal and Fate in Bioretention Cells. *J. Environ. Eng.* **2015**, *141*, 04014050. [CrossRef]
7. Paus, K.H.; Muthanna, T.M.; Braskerud, B.C. The hydrological performance of bioretention cells in regions with cold climates: Seasonal variation and implications for design. *Hydrol. Res.* **2016**, *47*, 291–304. [CrossRef]
8. Paus, K.H.; Braskerud, B.C. Forslag til dimensjonering og utforming av regnbed for norske forhold. *Vann.* **2013**, *1*, 54–67.
9. Gilbreath, A.; Mckee, L.; Shimabuku, I.; Lin, D. Multiyear Water Quality Performance and Mass Accumulation of PCBs, Mercury, Methylmercury, Copper, and Microplastics in a Bioretention Rain Garden. *J. Sustain. Water Built Environ.* **2019**, *5*, 1–10. [CrossRef]
10. Lefevre, G.H.; Novak, P.J.; Hozalski, R.M. Fate of naphthalene in laboratory-scale bioretention cells: Implications for sustainable stormwater management. *Environ. Sci. Technol.* **2012**, *46*, 995–1002. [CrossRef] [PubMed]
11. LeFevre, G.H.; Hozalski, R.M.; Novak, P.J. The role of biodegradation in limiting the accumulation of petroleum hydrocarbons in raingarden soils. *Water Res.* **2012**, *46*, 6753–6762. [CrossRef]
12. Roy-poirier, A.; Champagne, P.; Filion, Y. Bioretention processes for phosphorus pollution control. *Environ. Rev.* **2010**, *18*, 159–173. [CrossRef]
13. Brown, R.A.; Hunt, W.F. Improving bioretention/biofiltration performance with restorative maintenance. *Water Sci. Technol.* **2012**, *65*, 361–367. [CrossRef]
14. Roy-poirier, A.; Champagne, P.; Filion, Y. Review of bioretention system research and design: Past, present, and future. *J. Environ. Eng.* **2010**, *136*, 878–889. [CrossRef]
15. Kole, J.P.; Löhr, A.J.; Van Belleghem, F.G.A.J.; Ragas, A.M.J. Wear and tear of tyres: A stealthy source of microplastics in the environment. *Int. J. Environ. Res. Public Health* **2017**, *14*, 1265. [CrossRef]
16. Vogelsang, C.; Lusher, A.L.; Dadkhah, M.E.; Sundvor, I.; Umar, M.; Raneklev, S.B.; Eidsvoll, D.; Meland, S. *Microplastics in Road Dust—Characteristics, Pathways and Measures*; Norwegian Institute for Water Research: Oslo, Norway, 2018; 173p.
17. European Commission Directorate-General for Research and Innovation. *Environmental and Health Risks of Microplastic Pollution*; Publications Office of the European Union: Luxembourg, 2019. [CrossRef]
18. Kreider, M.L.; Sweet, L.I.; Panko, J.M.; McAtee, B.L.; Finley, B.L. Physical and chemical characterization of tire-related particles: Comparison of particles generated using different methodologies. *Sci. Total Environ.* **2009**, *408*, 652–659. [CrossRef]
19. Adachi, K.; Tainosho, Y. Characterization of heavy metal particles embedded in tire dust. *Environ. Int.* **2004**, *30*, 1009–1017. [CrossRef] [PubMed]
20. Cadle, S.H.; Williams, R.L. Gas and particle emissions from automobile tires in laboratory and field studies. *J. Air Pollut. Control Assoc.* **1978**, *28*, 502–507. [CrossRef]
21. Wagner, S.; Hüffer, T.; Klöckner, P.; Wehrhahn, M.; Hofmann, T.; Reemtsma, T. Tire wear particles in the aquatic environment—A review on generation, analysis, occurrence, fate and effects. *Water Res.* **2018**, *139*, 83–100. [CrossRef] [PubMed]
22. Andersson-Sköld, Y.; Johansson, M.; Gustafsson, M.; Järleskog, I.; Lithner, D.; Polukarova, M.; Strömvall, A.-M. *Microplastics from Tyre and Road Wear—A Literature Review*; Swedish National Road and Transport Research Institute: Linköping, Sweden, 2020. [CrossRef]
23. Smyth, K.; Drake, J.; Li, Y.; Rochman, C.; Van Seters, T.; Passeport, E. Bioretention cells remove microplastics from urban stormwater. *Water Res.* **2021**, *191*, 116785. [CrossRef]
24. Klöckner, P.; Seiwert, B.; Weyrauch, S.; Escher, B.I.; Reemtsma, T.; Wagner, S. Comprehensive characterization of tire and road wear particles in highway tunnel road dust by use of size and density fractionation. *Chemosphere* **2021**, *279*, 130530. [CrossRef]
25. Lange, K.; Magnusson, K.; Viklander, M.; Blecken, G.T. Removal of rubber, bitumen and other microplastic particles from stormwater by a gross pollutant trap—Bioretention treatment train. *Water Res.* **2021**, *202*, 117457. [CrossRef] [PubMed]
26. Lange, K.; Österlund, H.; Viklander, M.; Blecken, G.T. Occurrence and concentration of 20–100 µm sized microplastic in highway runoff and its removal in a gross pollutant trap—Bioretention and sand filter stormwater treatment train. *Sci. Total Environ.* **2022**, *809*, 151151. [CrossRef] [PubMed]
27. Haraldsen, T.K.; Gamborg, M.; Vike, E. *Utvikling av Jordblandinger til regnbed i Drammen Potteforsøk med Periodevis Vannmetning og Uttøking*; Norwegian Institute of Bioeconomy Research (NIBIO): Ås, Norway, 2019; Volume 5.
28. Statens Vegvesen. Vegkart. 2020. Available online: [https://vegkart-2019.atlas.vegvesen.no/#kartlag:geodata/hva:\(~\){\(farge:\T1\textquoteright0\\_0,id:643\)}/hvor:\(kommune:\(~\){602}\)/@243508,6627176,8/vegobjekt:1007532883:40a744:643](https://vegkart-2019.atlas.vegvesen.no/#kartlag:geodata/hva:(~){(farge:\T1\textquoteright0_0,id:643)}/hvor:(kommune:(~){602})/@243508,6627176,8/vegobjekt:1007532883:40a744:643) (accessed on 21 March 2021).
29. *Prosesskode 1: Standard Beskrivelse for Vegkontrakter*; Statens Vegvesen: Oslo, Norway, 2018.
30. Nilsen, V.; Christensen, E.; Myrmel, M.; Heistad, A. Spatio-temporal dynamics of virus and bacteria removal in dual-media contact-filtration for drinking water. *Water Res.* **2019**, *156*, 9–22. [CrossRef]

31. Mengistu, D.; Heistad, A.; Coutris, C. Tire wear particles concentrations in gully pot sediments. *Sci. Total Environ.* **2021**, *769*, 144785. [CrossRef]
32. Paus, K.H. Forslag til dimensjonerende verdier for trinn 1 i Norsk Vann sin tre-trinns strategi for håndtering av overvann. *Vannforeningen* **2018**, *1*, 66–77.
33. Unice, K.M.; Weeber, M.P.; Abramson, M.M.; Reid, R.C.D.; van Gils, J.A.G.; Markus, A.A.; Vethaak, A.D.; Panko, J.M. Characterizing export of land-based microplastics to the estuary—Part II: Sensitivity analysis of an integrated geospatial microplastic transport modeling assessment of tire and road wear particles. *Sci. Total Environ.* **2019**, *646*, 1650–1659. [CrossRef]
34. Mengistu, D.; Nilsen, V.; Heistad, A.; Kvaal, K. Detection and Quantification of Tire Particles in Sediments Using a Combination of Simultaneous Thermal Analysis, Fourier Transform Infra-Red, and Parallel Factor Analysis. *Int. J. Environ. Res. Public Health* **2019**, *16*, 3444. [CrossRef]
35. Baum, A.; Hansen, P.W.; Nørgaard, L.; Sørensen, J.; Mikkelsen, J.D. Rapid quantification of casein in skim milk using Fourier transform infrared spectroscopy, enzymatic perturbation, and multiway partial least squares regression: Monitoring chymosin at work. *J. Dairy Sci.* **2016**, *99*, 6071–6079. [CrossRef] [PubMed]
36. Thorpe, A.; Harrison, R.M. Sources and properties of non-exhaust particulate matter from road traffic: A review. *Sci. Total Environ.* **2008**, *400*, 270–282. [CrossRef]
37. Fernández-Berridi, M.J.; González, N.; Mugica, A.; Bernicot, C. Pyrolysis-FTIR and TGA techniques as tools in the characterization of blends of natural rubber and SBR. *Thermochim. Acta* **2006**, *444*, 65–70. [CrossRef]
38. Jusli, E.; Nor, H.M.; Jaya, R.P.; Zaiton, H. Chemical Properties of Waste Tyre Rubber Granules. *Adv. Mater. Res.* **2014**, *911*, 77–81. [CrossRef]
39. Ragn-Sells Gummigranulat. 2018. Available online: [https://www.ragnsells.no/globalassets/norge/dokumenter/dekkgjenvinning/rs\\_pb\\_granulat\\_fin\\_v5-2018-01-16.pdf](https://www.ragnsells.no/globalassets/norge/dokumenter/dekkgjenvinning/rs_pb_granulat_fin_v5-2018-01-16.pdf) (accessed on 2 August 2020).
40. Panko, J.M.; Chu, J.; Kreider, M.L.; Unice, K.M. Measurement of airborne concentrations of tire and road wear particles in urban and rural areas of France, Japan, and the United States. *Atmos. Environ.* **2013**, *72*, 192–199. [CrossRef]
41. Unice, K.M.; Kreider, M.L.; Panko, J.M. Comparison of tire and road wear particle concentrations in sediment for watersheds in France, Japan, and the United States by quantitative pyrolysis GC/MS analysis. *Environ. Sci. Technol.* **2013**, *47*, 8138–8147. [CrossRef] [PubMed]
42. Sommer, F.; Dietze, V.; Baum, A.; Sauer, J.; Gilge, S.; Maschowski, C.; Gieré, R. Tire abrasion as a major source of microplastics in the environment. *Aerosol Air Qual. Res.* **2018**, *18*, 2014–2028. [CrossRef]
43. Murphy, K.R.; Stedmon, C.A.; Graeber, D.; Bro, R. Fluorescence spectroscopy and multi-way techniques. PARAFAC. *Anal. Methods* **2013**, *5*, 6557–6566. [CrossRef]
44. Bro, R.; Kiers, H.A.L. A new efficient method for determining the number of components in PARAFAC models. *J. Chemom.* **2003**, *17*, 274–286. [CrossRef]
45. Besseling, E.; Quik, J.T.K.; Sun, M.; Koelmans, A.A. Fate of nano- and microplastic in freshwater systems: A modeling study. *Environ. Pollut.* **2017**, *220*, 540–548. [CrossRef]
46. Klöckner, P.; Seiwert, B.; Eisentraut, P.; Braun, U.; Reemtsma, T.; Wagner, S. Characterization of tire and road wear particles from road runoff indicates highly dynamic particle properties. *Water Res.* **2020**, *185*, 116262. [CrossRef]
47. Eisentraut, P.; Dümichen, E.; Ruhl, A.S.; Jekel, M.; Albrecht, M.; Gehde, M.; Braun, U. Two Birds with One Stone—Fast and Simultaneous Analysis of Microplastics: Microparticles Derived from Thermoplastics and Tire Wear. *Environ. Sci. Technol. Lett.* **2018**, *5*, 608–613. [CrossRef]
48. Baensch-Baltruschat, B.; Kocher, B.; Stock, F.; Reifferscheid, G. Tyre and road wear particles (TRWP)—A review of generation, properties, emissions, human health risk, ecotoxicity, and fate in the environment. *Sci. Total Environ.* **2020**, *733*, 137823. [CrossRef] [PubMed]
49. Hallberg, M.; Renman, G. Suspended solids concentration in highway runoff during summer conditions. *Polish J. Environ. Stud.* **2008**, *17*, 237–241.
50. Thomson, N.; McBean, E.; Mostrenko, I.B.; Snodgrass, W. Characterization of Stormwater Runoff from Highways. *J. Water Manag. Model.* **1994**, *6062*, 141–158. [CrossRef]
51. Alem, A.; Elkawafi, A.; Ahfir, N.D.; Wang, H.Q. Filtration of kaolinite particles in a saturated porous medium: Hydrodynamic effects. *Hydrogeol. J.* **2013**, *21*, 573–586. [CrossRef]
52. Conley, G.; Beck, N.; Riihimäki, C.A.; Tanner, M. Quantifying clogging patterns of infiltration systems to improve urban stormwater pollution reduction estimates. *Water Res. X* **2020**, *7*, 100049. [CrossRef]
53. Hanvey, J.S.; Lewis, P.J.; Lavers, J.L.; Crosbie, N.D.; Pozo, K.; Clarke, B.O. A review of analytical techniques for quantifying microplastics in sediments. *Anal. Methods* **2017**, *9*, 1369–1383. [CrossRef]
54. Imhof, H.K.; Schmid, J.; Niessner, R.; Ivleva, N.P.; Laforsch, C.; Imhof, H.K.; Schmid, J.; Laforsch, C.; Ivleva, N.P. A novel, highly efficient method for the separation and quantification of plastic particles in sediments of aquatic environments. *Limnol. Oceanogr. Methods* **2016**, *10*, 524–537. [CrossRef]
55. Karlsson, T.M.; Ekstrand, E.; Threapleton, M.; Mattsson, K.; Nordberg, K.; Hassellöv, M. *Undersökning av mikrokräp längs bohuslänska stränder och i Sediment*; University of Gothenburg: Kristineberg, Sweden, 2019.